

USING NIR TO PREDICT WOOD SHRINKAGE AND CELLULOSE CONTENT IN EUCALYPTUS NITENS

Toby Stovold, Mark Riddell, Sunita Jeram, Jaroslav Klápště, John Lee



Date: 30 March 2022

Publication No: SWP-R146

TABLE OF CONTENTS

EXECUTIVE SUMMARY	1
INTRODUCTION	2
AIM	2
METHODS – SHRINKAGE MODEL.....	2
Method and Materials.....	2
RESULTS – Shrinkage model.....	6
Discussion	6
METHOD – CELLULOSE MODEL.....	8
Methods and Materials.....	8
RESULTS – Cellulose Model	9
Discussion	9
CONCLUSION.....	10
ACKNOWLEDGEMENTS	10
REFERENCES	10
APPENDIX.....	12
Appendix 1- Lignin and carbohydrate results.....	12

Disclaimer

This report has been prepared by Scion for Forest Growers Research Ltd (FGR) subject to the terms and conditions of a research services agreement dated 1 January 2016.

The opinions and information provided in this report have been provided in good faith and on the basis that every endeavour has been made to be accurate and not misleading and to exercise reasonable care, skill and judgement in providing such opinions and information.

Under the terms of the Services Agreement, Scion's liability to FGR in relation to the services provided to produce this report is limited to the value of those services. Neither Scion nor any of its employees, contractors, agents or other persons acting on its behalf or under its control accept any responsibility to any person or organisation in respect of any information or opinion provided in this report in excess of that amount.

EXECUTIVE SUMMARY

The key outcome from this research is the ability to use predictions from NIR models for wood shrinkage and lignin/cellulose content as a substitute for expensive destructive phenotyping methods.

The evaluation was performed on wood samples retained from an open pollinated field experiment (“Keen’s block”) specifically to develop NIR based models for shrinkage based on previous data, and new wet chemistry determinations for lignin and wood sugars once funding allowed.

The NIR models developed explained up to 46% of the variation in tangential shrinkage and 26% of radial shrinkage in samples previously measured. They also explained 76% of the variation of Lignin, 32% of Galactose and 28% of Glucose. After applying the NIR models to 800 stored samples, and using the family information associated with the disks, estimated heritabilities for Lignin was 0.46, Galactose 0.29 and Glucose 0.3, which would allow the use of the models in the breeding program.

Having models which allows the prediction of shrinkage and cellulose from wood samples adds another option for screening and selecting the next generation of *E.nitens* in New Zealand, beyond the traditional method based on growth and form traits.

INTRODUCTION

In 2015 a *Eucalyptus nitens* growth stress and shrinkage study was carried out by destructively sampling a *E. nitens* progeny trial (FR491 planted 2007) at Southwood Export Ltd.'s "Keen's Block". That study was looking to quantify within the trial the level of variation for growth stress, and wood shrinkage (longitudinal, radial, and tangential) with a view to making new selections for seed orchards with improved wood properties. Results (Sountama, 2016) were promising and several new selections were identified and then grafted to Orchards.

The destructive sampling method commonly used to predict shrinkage, lignin, and cellulose is financially expensive, therefore at the time additional wood samples were collected and stored with the intent of future investigating the potential use of NIR (Near Infrared Spectroscopy) to make predictive models using non-destructive samples, such as increment cores. This report covers the results from using NIR to predict shrinkage, lignin, and cellulose content from the saved wood samples.

AIM

The aim of this study is to determine if NIR information from can be used to predict wood shrinkage, and cellulose in *E. nitens*.

Wood shrinkage is an important factor in lumber degrade, and a likely limiting factor in the use of in *E. nitens* for sawn timber products. Finding a method that does not require destructive sampling to obtain shrinkage information would allow the breeding program to select for individuals that exhibit lower levels of shrinkage for seed orchards. NIR information has also been successfully used to predict cellulose (Kube, 2011) as a substitute for Pulp Yield, a trait of significant economic importance which is expensive and difficult to measure using traditional wet chemistry methods at the breeding population level.

Two models, namely *Shrinkage Model* and *Cellulose Models* were investigated. Methods and results are described hereafter.

METHODS – SHRINKAGE MODEL

Method and Materials

From the previous study (Sountama, 2016), for each disk used to determine shrinkage, a paired disk was cut from the stem adjacent to the shrinkage disk (3m and 6m above ground). These disks were stored as half disks to prevent cracking, until funding became available for NIR scanning. In 2016 funding was available to scan 200 half disks, and a further 600 half disks in 2019.

Disk selection

Disks were selected randomly from the 3m samples, and from the second field collection where a matching line had been scribed with a chainsaw to assist with future alignment of the paired disks. Some disks were excluded from the selection pool, based on defects found in the original shrinkage block data. Selected disks were machined down to 20 mm thickness and conditioned over several weeks until moisture content stabilised to around 12%.

Scanning

All disks were scanned using the SCION Diskbot, which contains an automated NIR camera scanning in the range of 900 to 1700nm.

Pre-Processing NIR scans

Several steps were undertaken to prepare the NIR data before use, including

1. Removal of Bad pixels
2. Confirming alignment between the 2 disk halves (some required rotation)
3. Referencing signal to white/dark reference standards
4. Savitzky-Golay (1964) smoothing of reflectance data
5. Conversion to absorbance data- NIR data is reflectance
6. 14 outliers were identified and disks removed- these matched observational notes of defects such as resin pockets, branch traces
7. Standard normal variate transformation of absorbance spectra at the hyperspectral pixel level
8. Partitioning of the pixel level spectra into inner and outer zone
9. Averaging of transformed spectra at the inner disk area level
10. Averaging of transformed spectra at the outer disk area level

Data Matching

For each pair of disks scanned, matching data was assigned from the previous study (Sountama, 2016). Available data included density, moisture content, shrinkage (Longitudinal, Radial and Tangential, before and after steam reconditioning). The dimensions of the shrinkage blocks were also available. Each Matched disk contained data from 2 inner and 2 outer blocks (see Figure 1.) Radial dimensions of the inner and outer blocks was approximately half of the disk radius.

Figure 1. Picture of blocks cut in previous study showing location within disk and positioning of inner and outer blocks



Model development

Two-thirds of the data was partitioned off for model training, leaving one-third for testing of the models. Allocation to training or test sets was done at the family level to avoid overtraining the model. Additionally the training set was further partitioned into calibration and validation sets, and models were developed using leave-one-out cross validation to determine the number of components in the model. It was found that it was not always possible to match the orientation of both samples a decision was made to average the shrinkage data for the 2 inner block and 2 outer blocks, and then partition the disk scan pixels into 2 matching 'inner' and 'outer' zones the boundary of which was determined from the size of the inner block.

Two additional checks on data normality were made at this point by means of verifying that moisture content and density values were not showing any trends between the testing and training groups. No trends were observed on both moisture content (Figure 2) and density (Figure 3).

Figure 2- Moisture content of outer blocks sorted by family and data group (training or validation)

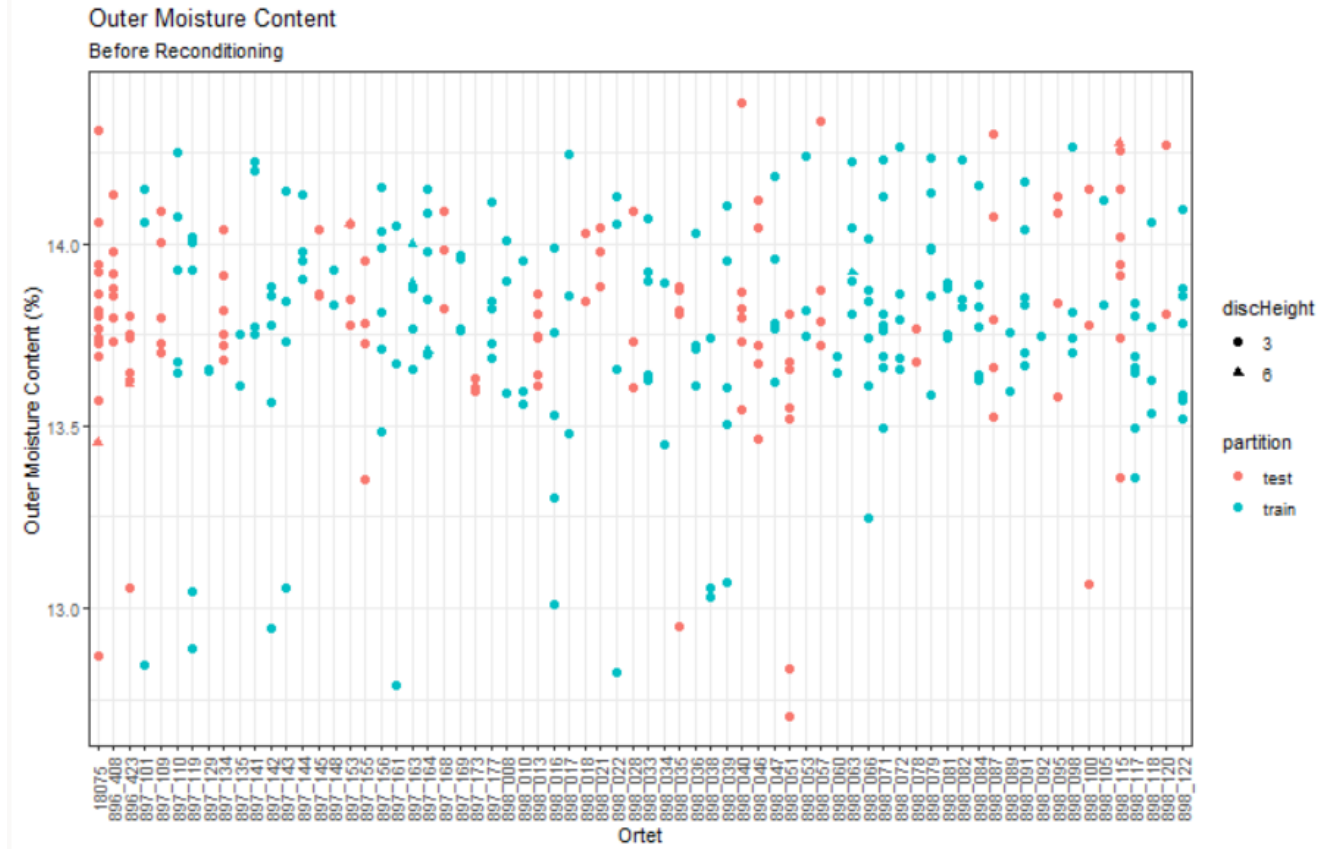
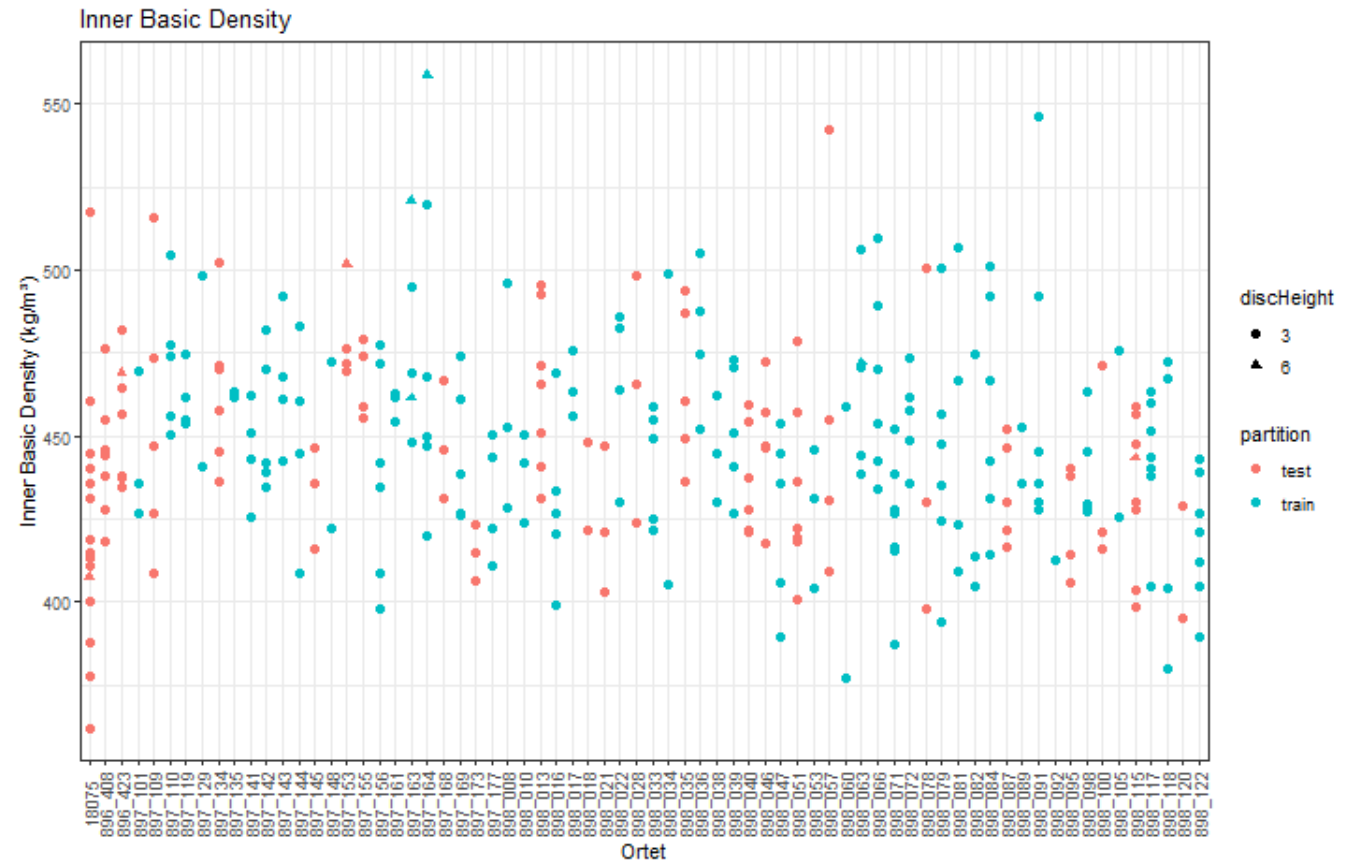


Figure 3- Density of inner blocks sorted by family and data group (training or validation)



First models developed was based on PLS (Partial least squares regression) using RStudio (*RStudio Team (2020)*) where the effects of each of the NIR components was considered one at a time, and the a second model developed (PLS2) which looked to maximise the interactions between components.

RESULTS – Shrinkage model

The amounts of variance explained by the second model are shown in Table 1. Summary statistics for all disks are shown in Table 2.

Table 1 Results from PLS2 model

Location and Shrinkage type	Variance explained (%) Before Reconditioning	Variance explained (%) After Reconditioning	Number of significant components before	Number of significant components after
Inner Block Longitudinal	7.8	6.2	2	1
Inner Block Radial	4.6	15.8	3	4
Inner Block Tangential	15.4	26.3	6	8
Outer Block Longitudinal	5.6	2.5	6	0
Outer Block Radial	13.6	28	5	6
Outer Block Tangential	24.9	46.5	8	7

Table 2 Nitens Shrinkage Percentage – Summary Statistics for all discs

These summary statistics are for the average measured block shrinkages – the two inner block results are averaged for each disc, and the two outer blocks are averaged for each disc

Shrinkage Measurement	Mean (%)	Standard deviation (%)	Minimum (%)	Maximum (%)
InnerLongitudinalBefore	0.04	0.09	-0.29	0.43
InnerRadialBefore	1.91	0.43	0.87	3.35
InnerTangentialBefore	5.94	0.95	4.34	11.46
InnerLongitudinalAfter	0.03	0.08	-0.24	0.35
InnerRadialAfter	1.57	0.29	0.74	2.83
InnerTangentialAfter	4.32	0.53	2.83	7.93
OuterLongitudinalBefore	-0.06	0.09	-0.63	0.25
OuterRadialBefore	4.31	1.19	1.57	9.52
OuterTangentialBefore	9.56	2.21	5.16	16.91
OuterLongitudinalAfter	-0.09	0.09	-0.62	0.38
OuterRadialAfter	2.39	0.48	0.73	4.55
OuterTangentialAfter	5.40	0.69	2.13	7.64

Discussion

Longitudinal shrinkage had the lowest amount of variation explained by the model, with 7.8% and 5.6% for inner and outer blocks respectively before reconditioning. Using data from the blocks after steam reconditioning, this reduced to 6.2% and 2.5%. This low prediction was not unexpected as in the original shrinkage study longitudinal data also gave the lowest heritability. Radial shrinkage was only slightly better at 4.6% and 13.6% before reconditioning. Model prediction improved after

reconditioning to 15.8% and 28%. The highest predictions were obtained for tangential shrinkage with 15.4% and 24.9% before reconditioning then improving to 26.3% and 46.5% after reconditioning.

It is worth noting that the two types of shrinkage (before and after reconditioning) represent different aspects of the drying process. Shrinkage before reconditioning includes normal differential shrinkage, caused by the cell wall losing moisture during drying, as well as collapse shrinkage, which is caused by the cell walls buckling and collapsing early in the drying process. Following reconditioning some of the collapse shrinkage is recovered, but in *E. nitens* there is often proportion of the collapse that is non-recoverable (i.e. cannot be removed by reconditioning), so it will still form a component of the shrinkage following reconditioning. It is also worth noting that the formation of recoverable collapse can cause within-ring internal checks, which cause irreversible damage to the wood, even if the collapse can be recovered by reconditioning. Because the after reconditioning values have a smaller collapse component, the higher percentage variance explained for the shrinkage after reconditioning suggests that the NIR model may be better able to predict differential shrinkage compared to collapse shrinkage, but further work would be needed to confirm this. While it may be possible to separate recoverable and non-recoverable collapse components from the shrinkage block data, from a tree breeding perspective, aiming to reduce both the shrinkage before reconditioning and shrinkage after reconditioning will reduce the overall propensity of the wood to collapse and form within-ring checks.

The model was subsequently tested on disks and boards saved from two previous sawing studies. These discs were also scanned with Diskbot, in an attempt to predict levels of internal checking and collapse in the sawn timber, from the levels of tangential shrinkage predicted in the discs (see SWP Technical report SWP-T145 "Using NIR to predict sawn timber quality in *E. nitens*" by R. Sargent and T. Stovold). The trees that produced timber with high levels of internal checking also tended to have the highest levels of predicted tangential shrinkage, but this correlation was not strong enough to predict the dried timber quality of boards cut from individual trees.

As a method of screening breeding populations, the model will give useful information for shrinkage, and 12mm increment cores can be substituted for disks meaning trials can be non-destructively sampled. Cores would be machined, removing coring artifacts such as surface staining to provide a suitable surface for scanning.

METHOD – CELLULOSE MODEL

Methods and Materials

To build a cellulose model, it was proposed to do wet chemistry on 30 disks and then relate the results to the NIR data to build a model. To select the disks, an existing cellulose and lignin model developed for Pinus Radiata was run on all disks already scanned (800). From these results, 40 disks were selected to allow rejects. The 40 disks selected covered the predicted range of cellulose and lignin estimates produced by applying the Pinus radiata model. The disks were recovered from storage and examined, and 3 disks were found to have defects and were not used in the study. To have more data to create the model, all 37 disks were used.

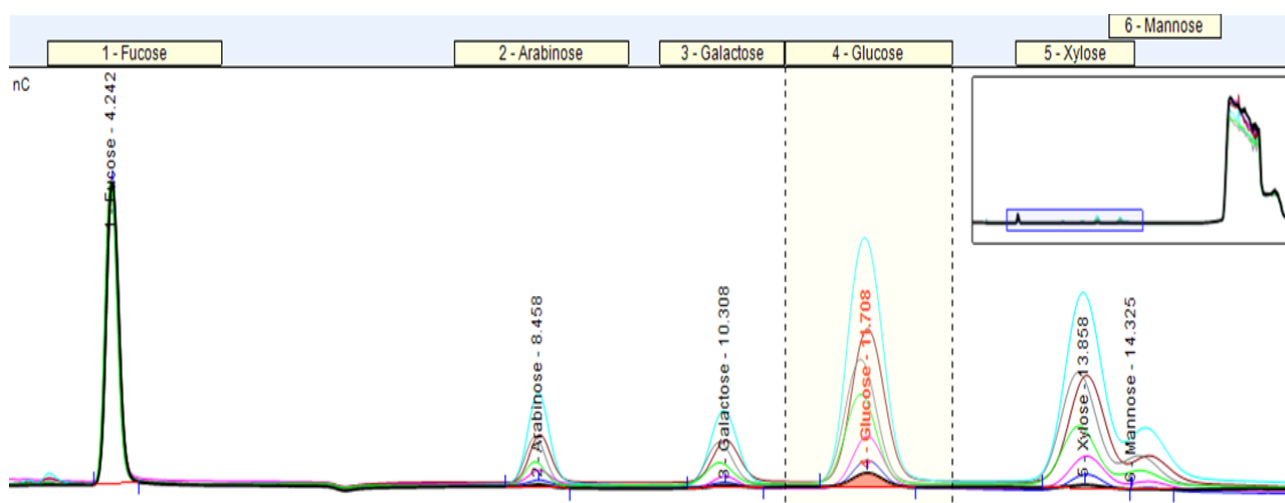
For all disks, a 15 mm strip was cut from bark to bark adjacent to the pith. The strip was then cut in half, one half was retained for future testing, and the other half ground to 20 mesh size using a Wiley Mill.

From each ground disk, 2 samples were taken which were then extracted in EtOH using Soxtec apparatus with a boiling time of 1 hour and rinsing time of 1 hour. The extracted samples were air dried in fume hood and placed in an oven at 55°C prior to lignin hydrolysis.

For the lignin and carbohydrate analysis, the extracted samples were digested using 72% sulphuric acid in a water bath at 30°C for 1 hour. They were then diluted to ~3% sulphuric acid and autoclaved for 1 hour at 121°C, 15 psi. Once autoclaved they were left to cool before being filtered onto pre-weighed GFA paper for acid-insoluble lignin. The filtrate was kept for acid-soluble lignin and carbohydrates. The acid soluble lignin was run the same day and was performed by taking the absorbance reading at 205 nm on a UV/Vis spectrophotometer. The carbohydrate analysis is performed by diluting the filtrate, adding fucose solution at 10ppm as an internal standard to ensure results are at the right scale, 0.22µm nylon filtering and running on a Dionex IC3000 instrument with eluent generation at 2mM KOH. Samples were run in batches of 12, each batch having 10 samples and 2 control samples.

As a quality control check, with every extractive size of the batch run, at least 2 x wood (mature pine/eucalyptus) quality control samples were taken through the entire process. Replicate analyses were performed on each submitted sample within each run to identify any abnormal results. Figure 4 shows a range of sample results from the chromatograph.

Figure 4. Typical chromatograms observed from seven Eucalyptus samples



RESULTS – Cellulose Model

Full results for each sample can be found in Appendix 1. In general amounts extracted for Lignin and the 5 carbohydrates (Arabinose, Galactose, Glucose, Xylose, and Mannose) were in the ranges expected and like other studies (Kube et al 2011). After some preliminary analysis it was decided there were a few outliers, and where there was a greater than 6% difference between replicates for glucose or galactose the data was not used for model generation. In total 5 samples were excluded. Models for each extractive and combined sugars were predicted using R packages Hyperspec, Prospectr (for pre data processing) and PLS. Models were initially developed as grams per 100 grams of oven dried wood. At this point it was decided to not model Mannose and Arbinose, as many of the samples had less than 1/10 of a percentage extracted.

Initial models for KlasonLignin explained 76% of the variation, in line with other published results (Kube et al, 2011). However, models for Glucose and Galactose were lower than expected at 28% and 32% respectively. There was some investigation as to potential causes, sample size, extraction run time and extraction chemical, but no obvious cause was identified.

To improve the models for the sugars, they were re-predicted as a percentage of total sugars rather than g/100g of oven dried wood. These models for Glucose and Galactose showed improved predictions at 78% and 60% respectively.

All models, including the re-predicted ones, were then applied to all 800 NIR scanned disks to create lignin and sugar values. Using the family information associated with the disks, these values were then used to create breeding values and calculate heritability's. Heritability's for inner wood, Lignin, Glucose and Galactose were estimated to be 0.46, 0.30 and 0.29 respectively. For the outerwood region heritabilty's increased to 0.54 for Lignin, and decreased to 0.16 for Glucose and 0.15 for Glactose. All heritability prections are shown in Table 3. There was however reasonable correlations between innerwood and outerwood. Correlations are shown in Table 4.

Table 3. Heritabilty predictions for Lignin and wood sugars

Trait	Heritability-Inner	Heritability-Outer
KlasonLignin	0.46	0.52
Galactose	0.29	0.15
Glucose	0.30	0.16
Xylose	0.32	0.3

Table 4. Correlations between inner wood and outer wood for Lignin and Wood sugars

		Outer			
		Klason Lignin	Galactose	Glucose	Xylose
Inner	Klason Lignin	0.687	-0.504	-0.529	0.373
	Galactose	-0.545	0.644	0.657	-0.123
	Glucose	-0.557	0.642	0.659	-0.143
	Xylose	0.276	-0.129	-0.148	0.726

Discussion

KlasonLigin in this study has a medium heritability, so reasonable genetic gains could be made selecting for or against in the breeding population. The Carbohydrates have medium-low heritabilities, so genetic gains for these would be more modest, but still worthwhile as combining the

carbohydrates gives a measure of cellulose content. Cellulose content can be used as a predictor of Kraft Pulp Yield(Downes et al. 2011) which is an important economic trait for *E. nitens* growers.

CONCLUSION

The use of NIR to predict traits traditionally measured by expensive destructive sampling offers the opportunity to include new traits into breeding and selection of *E. nitens* in New Zealand. One 12mm increment core could be collected from a tree and used to predict Lignin, Cellulose and Shrinkage. The same core would also be used for a density determination, and percentage heartwood. This offers several efficiencies. Pulp yield in Eucalyptus is an important economic trait and cellulose content can be used as a surrogate in making breeding and selection steps. Having models which allows prediction of shrinkage and cellulose add another option for screening and selecting the next generation of *E.nitens* in New Zealand.

ACKNOWLEDGEMENTS

Kane Fleet and Peter Bird for finding and preparing the samples for the wet chemistry determinations. Bernadette Nanayakkara for assisting with the laboratory work.

REFERENCES

Beleites, C. and Sergio, V. 2013. hyperSpec: a package to handle hyperspectral data sets in R', R package version 0.99-20200527 <https://github.com/cbeleites/hyperSpec>

Dowle, M., and Srinivasan, A. 2019. datatable: Extension of `data.frame`. R package version 1.12.8. <https://CRAN.R-project.org/package=data.table>

G M Downes , R Meder , H Bond , N Ebdon , C Hicks & C Harwood (2011) Measurement of cellulose content, Kraft pulp yield and basic density in eucalypt woodmeal using multisite and multispecies near infra-red spectroscopic calibrations, Southern Forests: a Journal of Forest Science, 73:3-4, 181-186, DOI: 10.2989/20702620.2011.639489

Eddelbuettel, D., Sanderson, C. 2014. RcppArmadillo: Accelerating R with high-performance C++ linear algebra. Computational Statistics and Data Analysis, Volume 71, March 2014, pages 1054-1063. URL <http://dx.doi.org/10.1016/j.csda.2013.02.005>

Fischer, B., Smith, M. and Pau, G. 2020. rhdf5: R Interface to HDF5. R package version 2.3.1. <https://github.com/grimbough/rhdf5>

Kube, P., Raymond, C.A. 2011 Genetic improvement of kraft pulp yield in Eucalyptus nitens using cellulose content determined by near infrared spectroscopy. Canadian Journal of Forest Research 34(11)

Mevik, B., Wehrens, R. and Liland, K. 2019. pls: Partial Least Squares and Principal Component Regression. R package version 2.7-2. <https://CRAN.R-project.org/package=pls>

RStudio Team (2020). *RStudio: Integrated Development for R*. RStudio, PBC, Boston, MA URL <http://www.rstudio.com/>.

Savitzky, A. and Golay M. J. E., "Smoothing and Differentiation of Data by Simplified Least Squares Procedures", *Anal. Chem.* 1964, 36, 8.

Stevens, A. and Ramirez-Lopez, L. 2020. An introduction to the *prospectr* package. R package Vignette R package version 0.2.0.

Suontama, M., Stovold, T., McKinley, R., Miller, M., Fleet, K., Low, C., & Dungey, H. (2016). *Selection for solid wood properties in Eucalyptus nitens*.

Zeileis, A. and Grothendieck, G. 2005. zoo: S3 Infrastructure for Regular and Irregular Time Series. *Journal of Statistical Software*, 14(6), 1-27. doi:10.18637/jss.v014.i06

APPENDIX

Appendix 1- Lignin and carbohydrate results

Lab sample ID	Client ID	EtOH Extractives %w/w od sample	%w/w extracted oven dried sample							
			Lignin		Neutral carbohydrates as anhydrosugars					Total
			Acid-insoluble (Klason)	Acid-Soluble	Arabinosyl units	Galactosyl units	Glucosyl units	Xylosyl units	Mannosyl units	
C00437	1	2.77	23.64	3.74	0.20	0.67	37.58	20.29	0.14	89.02
		2.34	22.97	4.24	0.24	0.70	38.62	20.85	0.13	90.09
C00438	2	2.05	20.69	4.14	0.17	0.69	42.35	19.41	0.13	89.63
		1.97	20.81	4.53	0.14	0.69	43.59	20.29	0.19	92.20
C00439	3	2.55	24.59	3.64	0.19	0.54	39.51	20.19	0.18	91.38
		2.51	23.62	3.97	0.15	0.64	39.76	20.27	0.23	91.15
C00440	4	1.29	22.11	4.42	0.15	0.84	42.82	18.31	0.11	90.06
		1.28	22.30	4.87	0.17	0.80	43.07	18.15	0.10	90.73
C00441	7	2.47	25.37	3.98	0.25	0.82	39.63	20.96	0.13	93.61
		2.54	25.41	3.82	0.25	0.90	40.41	20.71	0.16	94.20
C00442	8	2.54	23.89	3.98	0.20	0.66	35.98	20.11	0.35	87.70
		2.55	24.06	3.93	0.22	0.75	37.04	20.79	0.34	89.67
C00443	9	1.96	23.79	4.61	0.28	1.01	39.70	18.36	0.01	89.71
		1.90	23.17	4.51	0.26	1.18	40.24	18.51	0.03	89.80
C00444	10	3.11	23.91	4.01	0.24	0.59	36.61	20.46	0.30	89.22
		3.05	25.08	4.16	0.22	0.62	36.84	20.82	0.30	91.10
C00445	13	1.79	24.75	4.03	0.18	0.70	37.09	19.60	0.09	88.24
		1.92	25.21	4.00	0.18	0.65	37.18	19.61	0.05	88.81
C00446	14	2.95	24.61	4.24	0.20	0.64	37.12	21.38	0.21	91.35
		3.34	24.03	4.16	0.19	0.62	35.76	20.47	0.20	88.78
C00447	15	2.59	22.10	5.76	0.17	0.90	39.75	18.13	0.03	89.44
		2.55	21.63	5.45	0.11	0.79	41.04	18.37	0.07	90.00
C00448	16	2.75	23.27	4.72	0.09	0.83	38.06	19.56	0.09	89.38
		2.80	22.51	4.75	0.15	0.90	39.16	19.46	0.07	89.79
C00449	17	2.93	23.06	4.61	0.17	0.53	36.46	20.40	0.24	88.41
		3.06	23.99	4.56	0.13	0.52	38.05	20.88	0.33	91.52
C00450	18	2.47	22.30	4.23	0.15	0.82	39.30	18.99	0.15	88.39
		2.46	22.21	4.60	0.13	0.73	38.65	18.52	0.11	87.41
C00451	19	3.45	23.86	4.27	0.17	0.66	36.94	21.97	0.09	91.41
		3.49	23.78	4.21	0.16	0.66	35.32	20.94	0.06	88.60
C00452	22	2.91	22.74	6.18	0.14	0.96	37.45	17.27	0.07	87.73
		3.07	23.48	4.26	0.14	0.94	35.43	16.22	0.06	83.61
C00453	23	2.13	22.88	4.99	0.10	0.86	39.38	18.04	0.10	88.49
		2.06	23.41	4.01	0.42	0.59	35.54	17.66	0.09	83.78
C00454	24	3.14	26.43	5.53	0.49	0.67	41.55	21.19	0.21	99.20
		3.09	26.53	3.87	0.19	0.58	37.98	19.95	0.21	92.40
C00455	25	2.97	25.08	4.61	0.18	0.64	34.22	20.61	0.37	88.67
		2.82	24.68	4.70	0.14	0.51	34.61	20.59	0.39	88.43
C00456	26	2.44	24.64	4.83	0.18	0.67	37.47	18.12	0.17	88.52
		2.52	23.55	4.10	0.18	0.58	36.24	17.70	0.19	85.06
C00457	27	2.67	24.06	4.42	0.26	0.87	36.55	20.10	0.03	88.97
		3.15	24.20	4.72	0.25	0.72	38.29	20.31	0.00	91.64

C00458	28	3.13	23.46	4.83	0.25	0.57	37.68	20.79	0.12	90.84
		2.65	23.65	4.22	0.29	0.75	36.86	20.48	0.08	88.98
C00459	29	3.11	24.62	4.02	0.25	0.56	37.02	20.04	0.13	89.75
		3.23	25.02	3.88	0.24	0.61	36.53	19.94	0.10	89.56
C00460	30	2.81	24.69	4.07	0.24	0.68	37.84	21.11	0.08	91.52
		2.73	24.70	4.89	0.25	0.69	37.78	21.16	<0.01	92.21
C00461	31	3.00	22.48	3.68	0.29	1.19	40.49	18.65	<0.01	89.77
		2.97	23.04	4.09	0.21	1.01	38.99	18.07	<0.01	88.38
C00462	32	2.22	23.95	2.88	0.18	0.82	36.02	20.40	0.16	86.63
		2.46	24.07	2.96	0.18	0.62	38.75	21.26	0.04	90.33
C00463	34	2.81	26.11	3.82	0.21	0.62	37.48	20.31	<0.01	91.36
		2.78	26.03	3.27	0.20	0.66	39.33	21.26	<0.01	93.52
C00464	35	2.69	24.73	3.47	0.18	0.60	39.62	21.11	<0.01	92.40
		2.71	24.81	4.38	0.16	0.58	41.76	21.88	<0.01	96.28
C00465	36	2.22	23.94	3.06	0.20	0.91	40.09	19.36	<0.01	89.78
		2.24	22.90	3.02	0.22	0.94	43.16	20.91	<0.01	93.38
C00466	37	2.80	23.18	3.77	0.24	1.05	42.76	20.31	<0.01	94.12
		2.80	23.51	3.53	0.21	0.96	43.33	20.17	<0.01	94.51
C00467	41	3.18	23.46	3.76	0.20	0.48	36.97	17.71	0.19	85.95
		3.20	23.57	3.44	0.21	0.53	38.80	18.04	0.21	88.01
C00468	42	3.25	24.52	3.32	0.20	0.69	36.30	18.04	0.19	86.52
		3.32	24.48	3.34	0.20	0.71	42.15	20.44	0.19	94.84
C00469	43	2.76	23.00	3.63	0.10	0.85	41.73	19.38	0.13	91.57
		2.69	22.80	3.18	0.18	0.78	46.30	20.63	0.11	96.67
C00470	45	2.68	22.99	5.29	0.19	0.57	40.88	19.94	0.39	92.92
		2.57	23.93	4.49	0.19	0.63	41.68	19.88	0.49	93.85
C00471	46	3.38	23.25	3.64	0.28	1.14	43.75	18.53	0.13	94.11
		3.48	23.56	3.87	0.24	1.22	44.75	18.82	0.12	96.05
C00472	47	2.69	24.71	2.61	0.24	0.49	37.72	20.13	0.03	88.63
		2.97	24.63	1.96	0.25	0.46	37.05	19.78	0.07	87.16
C00473	48	4.18	22.80	3.25	0.31	0.87	40.33	17.87	<0.01	89.60
		2.89	22.37	3.60	0.22	0.81	39.91	17.79	<0.01	87.60